Journal of Colloid and Interface Science 405 (2013) 336–343

Contents lists available at SciVerse ScienceDirect

Journal of Colloid and Interface Science

www.elsevier.com/locate/jcis

Influence of the dielectrophoretic force in mixed electrical double layers

José Juan López-García [a], José Horno [a,*], Constantino Grosse [b,c]

[a] Departamento de Física, Universidad de Jaén, Campus Las Lagunillas, Ed. A-3, 23071 Jaén, Spain
[b] Departamento de Física, Universidad Nacional de Tucumán, Av. Independencia 1800, 4000 San Miguel de Tucumán, Argentina
[c] Consejo Nacional de Investigaciones Científicas y Técnicas, Av. Rivadavia 1917, 1033 Buenos Aires, Argentina

ARTICLE INFO

Article history:
Received 9 April 2013
Accepted 15 May 2013
Available online 31 May 2013

Keywords:
Mixed electrical double layers
Ionsize effect
Ion permitivity effect
Modified Poisson–Boltzmann equation

ABSTRACT

The equilibrium properties of a charged plane immersed in an aqueous electrolyte solution are examined using a generalized Poisson–Boltzmann equation that takes into account the finite ion size by modeling the solution as a suspension of polarizable insulating spheres in water. This formalism is applied to a general solution composed of two or more counterion species with different valences, sizes, and effective permittivity values. It is shown that, due to the dependence of the dielectrophoretic force on the ion size and effective permittivity value, the concentration of the smaller counterion strongly increases while that of the larger one decreases in the immediate vicinity of the charged surface. As a result the surface potential value strongly increases as compared to the usual modified Poisson–Boltzmann theory that only includes steric interactions among ions. This effect is particularly important in the case of mixtures of univalent and divalent counterions, being significant even for relatively low surface charge values.

1. Introduction

The existence of an electrical double layer around a solid object in contact with an aqueous electrolyte solution plays a crucial role in colloid and polymer science, biophysics, electrochemistry, medicine, and numerous separation technologies (e.g., water and waste water filtration, membrane filtration, protein and cell separation, immobilization of enzymes, etc.) [1–3]. This is why models of the electrical double layer structure are subjects of great interest. The theoretical model based on the Poisson–Boltzmann (PB) equation is an acknowledged and widely used description of the diffuse part of the equilibrium electric double layer. However, it is not difficult to point at a number of shortcomings of this theory such as: the finite size of the ions is neglected, interactions among ions and between the solid object and the ions are not taken into account, the permittivity of the medium is assumed to be constant, incomplete dissociation of the electrolyte is ignored, etc. [4].

Since the pioneering work by Bikerman [5], various attempts have been made to modify the classic PB equation so that the volume constraint can be accounted for; we direct the reader to Bazant et al. [6] for a historical background. All these works are based on two assumptions: ions have an effective ionic radius R_i so that the local ion concentration cannot surpass a finite value (the lower index i corresponds to the ion type) and an activity coefficient (γ_i) is introduced in order to take into account the ion size effects. While different expressions for the activity coefficient have been used [7], most of these works [8–10] describe the ion size with an adjustable constant which is the same for all ion types in the system.

These assumptions lead to the following main consequence: the ion density close to a charged interface cannot attain unrealistically high values, improving on the results predicted by PB equation. However, it still presents important shortcomings: the correction of the modified PB over the PB equation only appears at high surface charges and for high bulk electrolyte concentrations and, in order to fit experimental data, it is necessary to consider effective ionic radii much larger than the hydrated ionic radii, which is physically objectionable.

It should be noted that the above mentioned assumptions imply a restriction on the ability of ions to approach one another or the solid–liquid interface. However, a finite ion size also means that ions have a finite volume that can no longer be occupied by the suspending medium. In recent papers [11,12] we presented an extension of the modified PB equation considering that ions can be modeled as insulating spheres with a permittivity different from that of the surrounding medium. This led to the following modifications of the theoretical model:

- The presence of ions in the suspending medium modifies its permittivity. Moreover, since the ion concentration near a charged interface strongly depends on the distance to its surface, the electrolyte solution permittivity should also depend on this distance.

* Corresponding author. Fax: +34 953 212838.
E-mail address: jhorno@ujaen.es (J. Horno).

0021-9797/$ - see front matter © 2013 Elsevier Inc. All rights reserved.
http://dx.doi.org/10.1016/j.jcis.2013.05.036

– A variable permittivity of the electrolyte solution leads to the appearance of a new force term acting on an ion since charges tend to move into regions of higher permittivity (a consequence of the so called Born energy).
– The dielectric sphere representing an ion gets polarized by the local electric field and acquires a dipole moment. Therefore, an additional dielectrophoretic force acting on the dipole will appear wherever the local field is non-uniform.

The study was made assuming symmetric binary electrolyte solutions with equal effective ionic radii and permittivity values for both ionic species. The main consequence was the amplification of the steric effects predicted by the usual modified PB equation, even for reasonable effective ionic radii.

In the present work we extend the study to a general electrolyte solution composed by two or more counterion species with different valences, sizes, and effective permittivity values. We show that even relatively small size differences lead to strong changes of the local equilibrium ion concentrations near the charged interface mainly due to the strong dielectrophoretic force and its dependence on the counterion sizes and effective permittivities.

2. Theory

Let us to consider an infinite plane with a surface charge density σ_S immersed in an infinite solution made of m ionic species represented by insulating spheres with effective radius R_i, permittivity ε_i, signed valence z_i, and bulk concentration c_i^∞ (in mol per unit volume) with $i \in \{1,2,\ldots,m\}$, suspended in a continuous medium with permittivity ε_w (Fig. 1).

2.1. Permittivity of the solution

Due to the presence of the ions, the permittivity ε_e of the solution should depend on their concentrations and permittivity values. It can be determined using the Maxwell mixture formula [13], which is quite accurate over the whole concentration range when the dispersions have a lower permittivity than the suspending medium:

$$\varepsilon_e = \varepsilon_w \frac{1 + 2\sum_{i=1}^{m} \phi_i \frac{\varepsilon_i - \varepsilon_w}{\varepsilon_i + 2\varepsilon_w}}{1 - \sum_{i=1}^{m} \phi_i \frac{\varepsilon_i - \varepsilon_w}{\varepsilon_i + 2\varepsilon_w}} \tag{1}$$

In this expression ϕ_i is the local value of the volume fraction occupied by ions of species i:

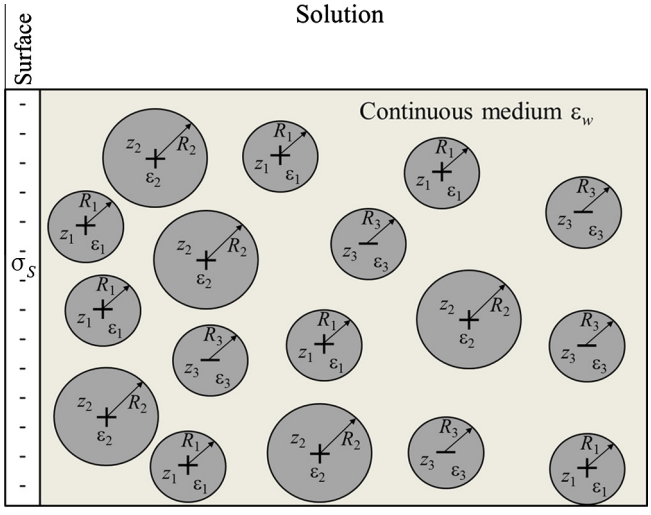

Fig. 1. Schematic representation of the considered system, see text.

$$\phi_i = \frac{4\pi}{3} N_A c_i R_i^3 \tag{2}$$

where c_i is the local concentration of ionic species i (in mol per unit volume) and N_A is the Avogadro number. Since the ion effective permittivity is lower than the permittivity of water (the permanent water molecule dipoles in the hydration layer are strongly oriented by the radial ionic field), the electrolyte solution permittivity decreases close to the charged plane where the total ion concentration increases.

Expression (1) is more general than the linear dependence of the electrolyte solution permittivity on the ion concentrations used in previous works [14,15], which can only be valid for low ion concentrations.

2.2. Poisson equation

The distribution of the electric potential, Ψ, is determined by the Poisson equation that must now be written taking into account the spatial dependence of the electrolyte solution permittivity:

$$\nabla \cdot (\varepsilon_e \vec{E}) = \varepsilon_e \nabla \cdot \vec{E} + \vec{E} \cdot \nabla \varepsilon_e = -\varepsilon_e \nabla^2 \Psi - \nabla \Psi \cdot \nabla \varepsilon_e = \rho = e N_A \sum_{i=1}^{m} z_i c_i \tag{3}$$

where ρ is the charge density, e is the elementary charge, and $\vec{E}$ is the electric field. Taking into account the plane geometry of the problem, Eq. (3) can be rewritten as:

$$\frac{d^2\Psi}{dx^2} = -\frac{eN_A}{\varepsilon_e} \sum\nolimits_{i=1}^{m} z_i c_i - \frac{d\ln\varepsilon_e}{dx} \frac{d\Psi}{dx} \tag{4}$$

2.3. Ionic concentrations

The ionic concentrations in the solution are determined by the following competing macroscopic average (per mol) forces acting upon the ions:

(i) The electric force:

$$\vec{F}_i^E = z_i e \vec{E} = -z_i e \nabla \Psi \tag{5}$$

This force attracts counterions towards the charged plane and repels co-ions. It only depends on the ion charge, being independent on their size and permittivity values.

(ii) The thermal force due to the random ion movement:

$$\vec{F}_i^T = -kT \nabla \ln\left(\frac{c_i}{c_i^\infty}\right) \tag{6}$$

where k is the Boltzmann constant and T is the absolute temperature of the system. Since the counterion concentration usually increases close to the charged plane while the co-ion concentration decreases, this force normally repels counterions from the plane while it attracts co-ions. It is independent of the ion size and permittivity values.

(iii) The steric force limiting the ability of ions to approach one another that appears when ion size effects are taken into account

$$\vec{F}_i^S = -kT \nabla \ln \gamma_i \tag{7}$$

where γ_i are the ionic activity coefficients. As in our previous works we use for simplicity, and for reasons to be discussed later on, a Bikerman [5] type expression for these coefficients:

$$\gamma_i = \frac{1}{1 - \frac{1}{p}\sum_{i=1}^{m}\phi_i} \tag{8}$$

where p is the packing coefficient ($p = 1$ for perfect packing, $p = \pi/3\sqrt{2} \approx 0.74$ for close packing, $p \approx 0.64$ for random close packing, $p = \pi/6 \approx 0.52$ for simple cubic packing). The steric force usually repels both counterions and co-ions away from the charged plane. It only depends on the ion sizes (the sizes of all the ion types), being independent of the ion charge and permittivity values.

(iv) The Born force that appears when the permittivity of the solution is allowed to change [16], since the electrostatic energy of an ion depends on the permittivity of the surrounding medium

$$\vec{F}_i^{B} = -\nabla\frac{\varepsilon_e}{2}\int_{R_i}^{\infty} E^2 dV = -\nabla\frac{z_i^2 e^2}{8\pi\varepsilon_e R_i} = -\frac{z_i^2 e^2}{8\pi R_i}\nabla\left(\frac{1}{\varepsilon_e}\right) \tag{9}$$

This force tends to move the ions to regions of higher permittivity repelling both counterions and co-ions from the charged plane. Its value strongly increases with the ion charge while it decreases with its size. It does not depend on the ion permittivity value.

(v) The dielectrophoretic force that appears when ions are assumed to behave as dielectric spheres, which become polarized acquiring an induced dipole moment $\vec{m}_i$. Therefore, wherever the local field is non-uniform, a dielectrophoretic force [17]

$$\vec{F}_i^{D} = (\vec{m}_i \cdot \nabla)\vec{E} = 2\pi\varepsilon_e R_i^3 \frac{\varepsilon_i - \varepsilon_e}{\varepsilon_i + 2\varepsilon_e}\nabla(E^2) \tag{10}$$

appears, which repels both counterions and co-ions from the charged plane since m_i is negative. This force is proportional to the ion volume and increases with decreasing ion permittivity value.

As can be seen, all the forces that depend on the finite ion size contribute to increase the double layer thickness.

2.4. Equilibrium potential and ionic concentrations

In equilibrium, the total force acting on the ions must vanish so that

$$\vec{F}_i^{E} + \vec{F}_i^{T} + \vec{F}_i^{S} + \vec{F}_i^{B} + \vec{F}_i^{D} = 0 \tag{11}$$

Using Eqs. (5)–(10), and taking into account the plane symmetry of the considered problem, the above equation reduces to:

$$\frac{d}{dx}\left[\ln\left(\frac{c_i}{c_i^{\infty}}\right) + \ln(\gamma_i) + \frac{z_i^2 e^2}{8\pi k T R_i}\frac{1}{\varepsilon_e} + \frac{z_i e}{kT}\Psi - \frac{2\pi R_i^3}{kT}\int \varepsilon_e \frac{\varepsilon_i - \varepsilon_e}{\varepsilon_i + 2\varepsilon_e}\frac{d^2}{dx}dx\right] = 0 \tag{12}$$

The solution of this equation is:

$$c_i = \frac{K_i}{\gamma_i}\exp(f_i)\exp\left(-\frac{z_i e\Psi}{kT}\right) \tag{13}$$

where K_i are integration constants, while

$$f_i = \frac{z_i^2 e^2}{8\pi k T R_i}\left(\frac{1}{\varepsilon_e^{\infty}} - \frac{1}{\varepsilon_e}\right) - \frac{4\pi e R_i^3}{kT}\int_x^{\infty}\frac{\varepsilon_e(\varepsilon_i - \varepsilon_e)}{\varepsilon_i + 2\varepsilon_e}\frac{d\Psi}{dx}\frac{d^2\Psi}{dx^2}dx \tag{14}$$

and

$$\varepsilon_e^{\infty} = \varepsilon_w \frac{1 + 2\sum_{i=1}^{m}\phi_i^{\infty}\frac{\varepsilon_i - \varepsilon_w}{\varepsilon_i + 2\varepsilon_w}}{1 - \sum_{i=1}^{m}\phi_i^{\infty}\frac{\varepsilon_i - \varepsilon_w}{\varepsilon_i + 2\varepsilon_w}} \tag{15}$$

where

$$\phi_i^{\infty} = \frac{4\pi}{3}N_A c_i^{\infty} R_i^3 \tag{16}$$

2.5. Boundary conditions

In order to complete the theoretical model, we use the following boundary conditions:

(1) The Gauss law relating the surface charge density on the plane to the normal component of the electric field

$$\left.\frac{d\Psi(x)}{dx}\right|_{x=0} = -\frac{\sigma_s}{\varepsilon_e(x=0)} \tag{17}$$

(2) The origin of the electric potential at $x \to \infty$,

$$\Psi(x \to \infty) = 0 \tag{18}$$

(3) The requirement that the ionic concentrations attain their bulk concentrations at $x \to \infty$

$$c_i(x \to \infty) = c_i^{\infty} \tag{19}$$

These conditions make it possible to determine the integration constants:

$$K_i = \frac{1}{1 - \frac{1}{p}\sum_{i=1}^{m}\phi_i^{\infty}}c_i^{\infty} = \gamma_i^{\infty}c_i^{\infty} \tag{20}$$

Combining this result with Eqs. (2) and (13) leads to

$$\phi_i = \frac{4\pi N_A}{3}\frac{\gamma_i^{\infty}}{\gamma_i}c_i^{\infty}R_i^3\exp(f_i)\exp(-z_i y) \tag{21}$$

where

$$y = \frac{e\Psi}{kT} \tag{22}$$

is the dimensionless electric potential. Using Eq. (8), the ionic concentrations finally become:

$$c_i = \frac{\gamma_i^{\infty}c_i^{\infty}\exp(f_i)\exp(-z_i y)}{1 + \frac{4\pi N_A\gamma_i^{\infty}}{3}\frac{1}{p}\sum_{j=1}^{m}c_j^{\infty}R_j^3\exp(f_j)\exp(-z_j y)} \tag{23}$$

2.6. Numerical solution

For computational reasons it is convenient to use the spatial variable

$$q = \exp(-\kappa x) \tag{24}$$

that confines the problem into a finite region, where

$$\kappa = \sqrt{\frac{e^2 N_A\sum_{i=1}^{m}z_i c_i^{\infty}}{kT\varepsilon_e^{\infty}}} \tag{25}$$

is the reciprocal Debye length. This transforms the theoretical model into:

$$\frac{d^2y}{dq^2} = -\frac{\varepsilon_e^{\infty}\gamma_i^{\infty}\sum_{i=1}^{m}z_i c_i^{\infty}\exp(f_i)\exp(-z_i y)}{\gamma_i\varepsilon_e q^2\sum_{i=1}^{m}z_i^2 c_i^{\infty}} - \left(\frac{d\ln\varepsilon_e}{dq} + \frac{1}{q}\right)\frac{dy}{dq} \tag{26}$$

where ε_e is defined in Eq. (1), and

$$f_i = \frac{z_i^2 e^2}{8\pi k T R_i}\left(\frac{1}{\varepsilon_e^{\infty}} - \frac{1}{\varepsilon_e}\right) - \frac{4\pi k T\kappa^2 R_i^3}{e}\int_q^0 \frac{\varepsilon_e(\varepsilon_i - \varepsilon_e)}{\varepsilon_i + 2\varepsilon_e} \times \frac{dy}{dq}\left[q^2\frac{d^2y}{dq^2} + q\frac{dy}{dq}\right]dq \tag{27}$$

These equations were solved using a finite differences scheme, i.e., discretizing the spatial variable q. Then the following algorithm was used:

1. The starting point is the solution of Eq. (26) for an uncharged plane: $\Psi(q) = 0, f_i(q) = 0, c_i(q) = c_i^{\infty}$ and $\varepsilon_e(q) = \varepsilon_e^{\infty}$.

2. The charge on the plane is slightly increased:
   2.1. Eq. (26) is linearized and solved using the previous values for $f_i(q)$, $c_i(q)$ and $\varepsilon_e(q)$;
   2.2. Eq. (21) is used to calculate ϕ_i;
   2.3. These values are used to calculate new values of $\varepsilon_e(q)$ using Eq. (1);
   2.4. These values are used to calculate new values of $f_i(q)$ using Eq. (27);
   2.5. Points 2.1–2.4 are repeated until convergence is attained.

3. Point 2 is repeated until the desired surface charge is attained.

It must be noted that because the variable y changes rapidly near the charged interface ($q = 1$), an appropriate simulation space grid must be modeled. In this work, the q-space grid is automatically adapted to the evolution of the potential profiles. If, during the simulation, strong changes of y with q are detected in any region of the q coordinate, more grid points are added into this region to ensure good accuracy and moderate CPU times.

3. Results and discussion

The calculations were performed considering an infinite plane with surface charge density $\sigma_S < 0$ in contact with different aqueous electrolyte solutions (typical values for the ion parameters are given in Table 1). Hydrated ionic radii and permittivity values have been taken from references [18,19], respectively. It should be noted that the ion permittivity values decrease with the valence modulus due to the increase of the permanent water molecule dipole orientation in the hydration shell.

The remaining system parameters are given in Table 2. Note that for sake of simplicity we did not take into account, just as done in [7], the existence of a minimum approach distance of ions to the charged plane.

3.1. Two univalent counterion types and equal bulk concentrations

We first consider an aqueous 5 mM LiCl and 5 mM CsCl electrolyte solution. Fig. 2 shows the counterion concentration profiles for different model approximations. The blue line represents the classical PB solution. Since this solution is solely determined by the electric and thermal forces, the Li^+ and Cs^+ densities coincide. The red line represents the modified PB solution that additionally includes the steric interactions among ions. The counterion concentrations no longer grow to unreasonably high values but rather attain saturation values that are related to the finite ion size. These

Table 1
Parameter values for different ionic species.

Ion	z_i	R_i (Å)	$\varepsilon_i/\varepsilon_0$
Li^+	1	3.82	25
Cs^+	1	3.29	25
Na^+	1	3.58	25
H^+	1	2.82	25
Ca^{++}	2	4.12	7
Cl^-	−1	3.32	25
OH^-	−1	3	25

Table 2
Parameter values used in the simulation except when indicated otherwise.

$e = 1.602 \times 10^{-19}$ C	$N_A = 6.022 \times 10^{23}$ mol^{-1}	$k = 1.381 \times 10^{-23}$ J/K
$T = 298$ K	$\varepsilon_w = 80 \cdot \varepsilon_0$	$p = 0.7405$

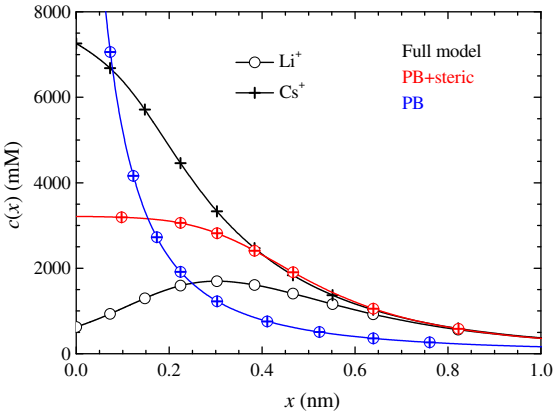

Fig. 2. Counterion concentration profiles for an aqueous 5 mM LiCl and 5 mM CsCl electrolyte solution and a 0.4 C/m^2 surface charge. Used parameter values given in Tables 1 and 2.

values can be derived from Eq. (23), setting $f_i = 0$ (in order to suppress all effects related to the ion and the electrolyte solution permittivities) and considering that the surface potential is negative and very high (in modulus):

$$c_{Li}^{sat} = \frac{3p}{4\pi N_A}\frac{c_{Li}^{\infty}}{c_{Cs}^{\infty}R_{Cs}^3 + c_{Li}^{\infty}R_{Li}^3} = \frac{3p}{4\pi N_A}\frac{1}{R_{Cs}^3 + R_{Li}^3} \tag{28}$$

$$c_{Cs}^{sat} = \frac{3p}{4\pi N_A}\frac{c_{Cs}^{\infty}}{c_{Cs}^{\infty}R_{Cs}^3 + c_{Li}^{\infty}R_{Li}^3} = \frac{3p}{4\pi N_A}\frac{1}{R_{Cs}^3 + R_{Li}^3} \tag{29}$$

where the second equalities result from the consideration that LiCl and CsCl have equal bulk concentrations. Note that the Bikerman Eq. (8) leads to saturation values that depend on the volume fraction occupied by all the ion species rather than the individual ion sizes corresponding to each of these species. Because of this, the Li^+ and Cs^+ concentrations are the same close to the charged plane. While this behavior constitutes a shortcoming of the Bikerman equation, and other more elaborate equations that solely depend on the volume fraction occupied by all the ions [20], we still used this equation because it made it possible to study the different counterion size effects solely related to the ion and electrolyte solution permittivities.

The black lines in Fig. 2 represent the results predicted by the full theory presented in this work that considers ions as dielectric spheres. The Born and dielectrophoretic forces tend to lower the counterion concentration: the Born force pulls ions to regions of higher permittivity while the dielectrophoretic force pulls ions to regions of lower electric field (because the induced dipole moment of the dielectric sphere representing the ion is negative). Because of this, full counterion saturation is no longer attained and, furthermore, the Li^+ and Cs^+ concentrations close to the charged plane no longer coincide. The Cs^+ concentration surpasses the Li^+ concentration because the repelling dielectrophoretic force acting on the Cs^+ ions is smaller due to their smaller size. The Born force has a qualitatively opposite dependence on the ion size: it is smallest for the largest ion. However this dependence is weaker for the Born (proportional to R_i^{-1}) than for the dielectrophoretic force (proportional to R_i^3). Furthermore, for relatively large ions the Born force is much weaker than the dielectrophoretic force.

Fig. 3 shows the dimensionless electric potential profiles for the different model approximations (left ordinate) and the relative electrolyte solution permittivity profile corresponding to the full theory (right ordinate). The classical PB solution, blue line, leads to the lowest potential because the corresponding double layer thickness is lowest, Fig. 2. When the steric force is incorporated

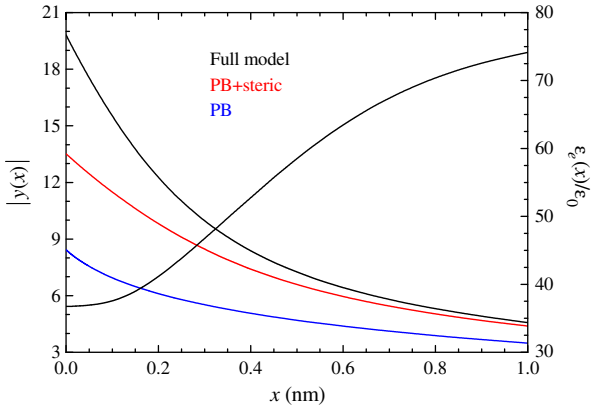

Fig. 3. Dimensionless electric potential profiles for an aqueous 5 mM LiCl and 5 mM CsCl electrolyte solution and a 0.4 C/m^2 surface charge (left ordinate); relative electrolyte solution permittivity profile corresponding to the full model (right ordinate). Used parameter values given in Tables 1 and 2.

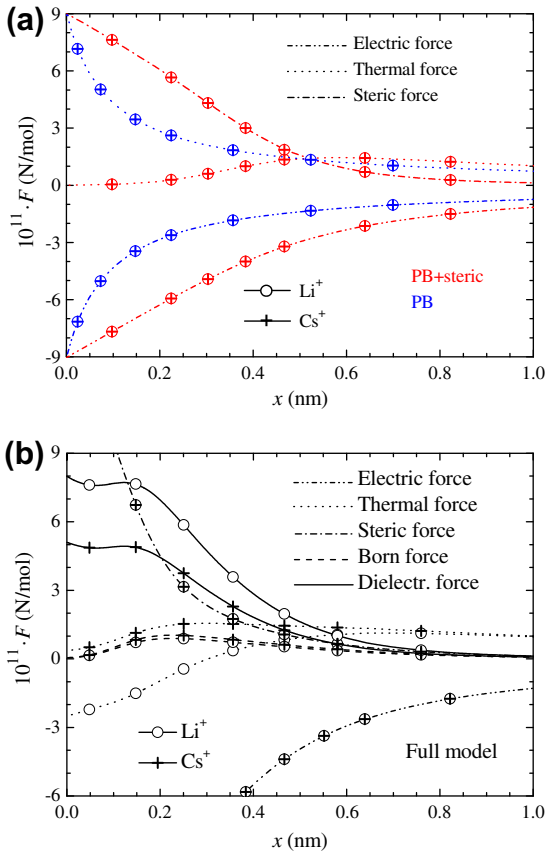

Fig. 4. Different molar force profiles for an aqueous 5 mM LiCl and 5 mM CsCl electrolyte solution and a 0.4 C/m^2 surface charge. (a) Poisson–Boltzmann and Poisson–Boltzmann with steric interactions among ions. (b) Full model. Used parameter values given in Tables 1 and 2.

into the model, red line, the potential increases due to the lowering of the counterion concentration, Fig. 2, and the corresponding increase of the double layer thickness required to neutralize the fixed surface charge. However, the slopes of the blue and red curves at the charged plane remain equal to one another because both the surface charge and the electrolyte solution permittivity have the same value for these two models, Eq. (17).

The electric potential further increases for the full model, black line, because of two effects: firstly the repulsive Born and dielectrophoretic forces that lower the thickness of the saturation zone increasing the total double layer thickness and, secondly, the electrolyte solution permittivity that strongly decreases inside the double layer due to the excluded ion volume. The low permittivity value close to the charged plane also determines the higher initial slope of the black line as compared to the red and blue ones.

Fig. 4 shows the profiles of the different force terms. For clarity, it was separated into two parts: Fig. 4a shows the results corresponding to the PB and the modified PB including just the steric force equations, while Fig. 4b shows all the forces corresponding to the full theory.

The blue lines in Fig. 4a represent the attractive electric and the repulsive thermal forces corresponding to the PB solution. Both forces exactly compensate each other and have the same values for both counterion types. Adding the steric interaction, red lines, increases the electric force modulus everywhere except at the interface, because the double layer becomes thicker decreasing the screening of the surface charge. For this same reason, the thermal force also increases far from the charged surface. However, at shorter distances, this force strongly decreases and finally vanishes because of the almost constant counterion concentration near the interface. On the contrary, the steric force attains its highest value at the interface despite this concentration plateau, because the activities diverge when the concentrations tend to their maximum values, Eq. (8). All these forces still have the same values for both counterion types.

Fig. 4b represents all the forces corresponding to the full model. The attractive electric force becomes even stronger mainly because the Born and dielectrophoretic forces being repulsive increase the thickness of the double layer. The other reason is the decrease of the electrolyte solution permittivity, Fig. 3, because of which the electric force at the charged surface attains a much higher value than in Fig. 4a. This and the repulsive steric force are the only ones that have the same values for both counterion types. On the contrary, thermal forces split into two lines because of the different counterion concentrations, Fig. 2. Note that for the larger Li^+ ion the thermal force becomes attractive close to the interface where the corresponding concentration, Fig. 2, increases with distance. The Born forces are rather weak for both counterion types due to their relatively large size, Eq. (9), attaining their maxima at distances where the electrolyte solution permittivity strongly changes, Fig. 3. This force is always slightly stronger for Cs^+ than Li^+ because the former ion is smaller than the latter. Finally, the strongest changes with respect to Fig. 4a are due to the repulsive dielectrophoretic force, which is strongest for the Li^+ ion because of its larger size. Close to the charged plane these forces first decrease with distance because the counterion concentration saturates leading to a constant volume charge density while the electrolyte solution permittivity remains constant. Therefore the electric field decreases linearly with distance so that the $\nabla(E^2)$, Eq. (10), decreases with distance. The increment of the dielectrophoretic forces that follows is due to the increase of the electrolyte solution permittivity while the final drop results from the decrease of the derivative of the electric field due to the lowering of the volume charge density.

Fig. 5 shows the dependence of the dimensionless surface potential on the surface charge density. The potential values along the right ordinate correspond to σ_s = 0.4 C/m^2 that is the value used in Figs. 2–4. As can be seen, steric effects are dominant at high surface charge values when the counterion concentration attains saturation close to the interface. The surface potential further increases mainly due to the dielectrophoretic force when the full model is considered, because the thickness of the double layer increases even more. Note, however, that for relatively low surface charge values, when saturation due to steric forces is not attained,

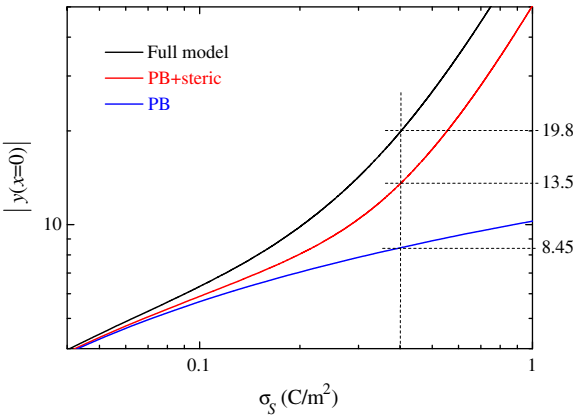

Fig. 5. Dimensionless surface potential as a function of the surface charge for an aqueous 5 mM LiCl and 5 mM CsCl electrolyte solution. The potential values along the right ordinate correspond to the surface charge used in Fig. 4. Used parameter values given in Tables 1 and 2.

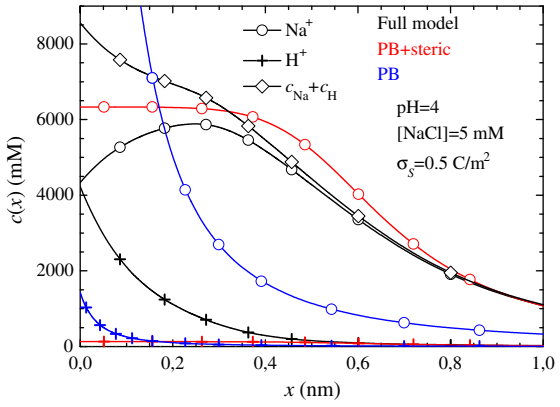

Fig. 6. Counterion concentration profiles for an aqueous 5 mM NaCl electrolyte solution at pH = 4 and a 0.5 C/m^2 surface charge. The black line with diamonds represents the total counterion concentration predicted by the full model. Used parameter values given in Tables 1 and 2.

the dielectrophoretic force becomes the main reason for the increment of the surface potential with respect to the PB solution.

3.2. Two univalent counterion types and different bulk concentrations

We next consider a system with two univalent counterions that widely differ both in size and in bulk concentration: an aqueous 5 mM NaCl solution at pH = 4, which implies a 0.1 mM bulk concentration of H^+ ions. In order to obtain stronger effects, the surface charge was increased to a still reasonable 0.5 C/m^2 value. Fig. 6 shows the obtained concentration profiles.

The PB theory, blue lines, leads to unreasonably high Na^+ and small H^+ concentrations close to the charged plane. These concentrations only depend on the ion charges and bulk concentrations being independent of the ion sizes.

The modified PB theory including steric effects, red lines, leads to a strong saturation of the counterion concentration that expands the double layer. As in the previous case, ion saturation values, Eqs. (28) and (29), only depend on the total excluded ion volume in the bulk rather than the individual ion sizes. However, these saturation concentrations are not equal anymore because the bulk concentrations differ from one another:

$$c_{\mathrm{Na}}^{sat} = \frac{3p}{4\pi N_A}\frac{c_{\mathrm{Na}}^{\infty}}{c_{\mathrm{Na}}^{\infty}R_{\mathrm{Na}}^3 + c_{\mathrm{H}}^{\infty}R_{\mathrm{H}}^3} = \frac{3p}{4\pi N_A}0.0216 \tag{30}$$

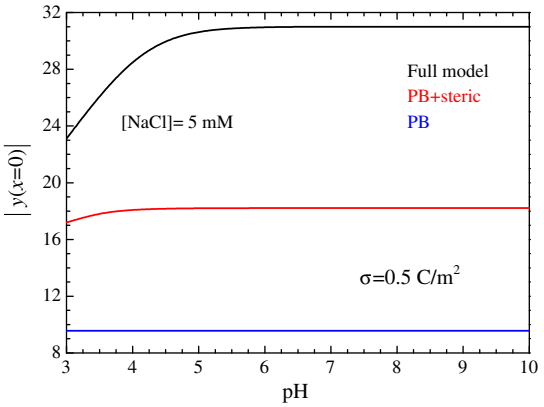

Fig. 7. Dimensionless surface potential as a function of the pH for an aqueous 5 mM NaCl electrolyte and a 0.5 C/m^2 surface charge. Remaining parameters given in Tables 1 and 2.

$$c_{\mathrm{H}}^{sat} = \frac{3p}{4\pi N_A}\frac{c_{\mathrm{H}}^{\infty}}{c_{\mathrm{Na}}^{\infty}R_{\mathrm{Na}}^3 + c_{\mathrm{H}}^{\infty}R_{\mathrm{H}}^3} = \frac{3p}{4\pi N_A}0.000432 \tag{31}$$

The full model, black lines, shows that the repelling dielectrophoretic force that is much stronger for Na^+ than H^+ ions because of their much larger size, leads to a strong decrement of the Na^+ concentration near the plane and a corresponding increment of the H^+ concentration. The sum of these two concentrations shows that the total counterion concentration is saturated but no longer uniform: it increases close to the interface because H^+ ions can be packed more densely than Na^+ ions. It should be noted that this behavior has been achieved despite the use of the Bikerman equation for the steric interaction, Eq. (8), which does not favor the increase of the smallest ion concentration near the charged plane. Actually, the full model concentrations are quite similar to the results presented in [7] where a PB theory modified by means of an activity expression that does take into account the individual ion sizes [21,22] was used. It is remarkable that the inclusion of the Born and the dielectrophoretic forces results in a similar behavior.

Fig. 7 shows the dependence of the dimensionless surface potential on the pH keeping constant the surface charge at the same value as in Fig. 6: 0.5 C/m^2. The PB solution, blue line, is practically independent of the pH value since the bulk H^+ concentration remains much smaller than the Na^+ concentration over the whole considered pH range. The modified PB theory including steric interactions among ions, red line, shows a slight decrease of the surface potential at the lowest pH values. Its origin can be explained considering the total counterion saturation concentration:

$$\begin{aligned} c_{\mathrm{Na}}^{sat} + c_{\mathrm{H}}^{sat} &= \frac{3p}{4\pi N_A}\frac{c_{\mathrm{Na}}^{\infty} + c_{\mathrm{H}}^{\infty}}{c_{\mathrm{Na}}^{\infty}R_{\mathrm{Na}}^3 + c_{\mathrm{H}}^{\infty}R_{\mathrm{H}}^3} \\ &\approx \frac{3p}{4\pi N_A R_{\mathrm{Na}}^3}\left[1 + \frac{c_{\mathrm{H}}^{\infty}}{c_{\mathrm{Na}}^{\infty}}\left(1 - \frac{R_{\mathrm{H}}^3}{R_{\mathrm{Na}}^3}\right)\right] \end{aligned} \tag{32}$$

which increases with c_{H}^{∞} because R_{H} is smaller than R_{Na}. Therefore, a smaller double layer thickness is required in order to neutralize the surface charge leading to a lower surface potential.

Finally, the surface potential dependence on pH strongly increases when the full model is considered. This is mainly due to the repelling dielectrophoretic force and its dependence on the ion size: much stronger for Na^+ than H^+ ions. This increases the H^+ concentration close to the charged plane lowering even more the thickness of the double layer and, therefore, the surface potential.

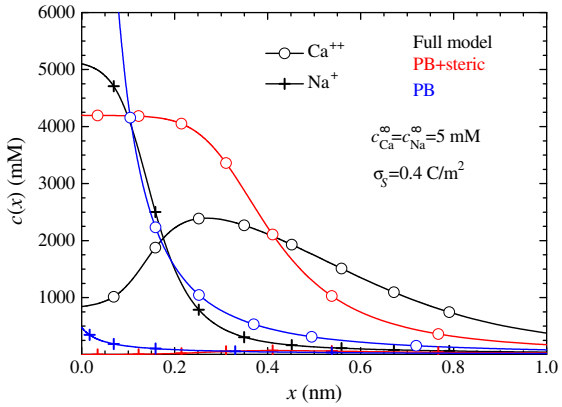

Fig. 8. Counterion concentration profiles for an aqueous 5 mM NaCl and 5 mM $CaCl_2$ electrolyte solution and a 0.4 C/m^2 surface charge. Used parameter values given in Tables 1 and 2.

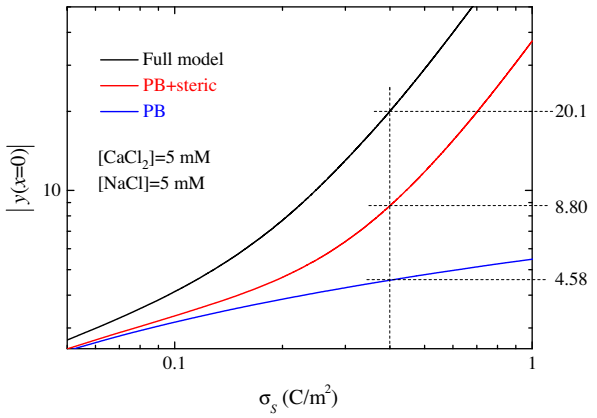

Fig. 9. Dimensionless surface potential as a function of the surface charge for an aqueous 5 mM NaCl and 5 mM $CaCl_2$ electrolyte solution. The potential values along the right ordinate correspond to the surface charge used in Fig. 8. Used parameter values given in Tables 1 and 2.

3.3. One univalent and one divalent counterion type and equal bulk concentrations

We finally consider a 5 mM NaCl and 5 mM $CaCl_2$ mixture. Fig. 8 shows the counterion concentration profiles for different model approximations. The blue line represents the classical PB solution. Since the electric attractive force is two times higher for Ca^{++} than for Na^+ ions, the counterion population near the plane is made almost exclusively of Ca^{++} ions that attain unreasonably high values.

The red line represents the modified PB solution that additionally includes the steric interactions among ions. The counterion concentrations no longer grow to unreasonably high values but rather attain saturation values that are related to the finite ion sizes. These values can be derived from Eq. (23) just as in the case of Eqs. (28) and (29), setting f_i to zero and considering that the potential is very high and negative. This leads to:

$$c_{\mathrm{Ca}}^{sat} = \frac{3p}{4\pi N_A R_{\mathrm{Ca}}^3} \tag{33}$$

$$c_{\mathrm{Na}}^{sat} = 0 \tag{34}$$

showing that the univalent Na^+ ions are fully expelled from the saturation layer that is exclusively made of divalent Ca^{++} ions.

Finally the black lines correspond to the full model that represents the ions as dielectric spheres. The main difference with respect to the previous cases is that this theory includes repelling dielectrophoretic forces that are much higher for Ca^{++} than for Na^+, not because of the size difference as in the previously considered cases, but due to the huge permittivity difference: 7 for divalent versus 25 for univalent ions. Far from the plane the field is weak and the electric force is stronger than the dielectrophoretic force because the former is linear in the field while the latter, Eq. (10), depends on the field squared. This is also the reason why the dielectrophoretic force can become stronger than the electric force close to the plane where the field is much stronger. Because of this, the Na^+ ion concentration surpasses the concentration of Ca^{++} ions in the immediate neighborhood of the charged plane.

Fig. 9 shows the dependence of the surface potential on the surface charge. The potential values along the right ordinate correspond to $\sigma_s = 0.4$ C/m^2 that is the value used in Fig. 8. The large increment of the surface potential due to the inclusion of the steric interaction among ions (difference between the red and blue lines) is due to the saturation of the counterion concentration close to the charged plane and the corresponding increase of the double layer thickness. However, the full model that further represents the ions as dielectric spheres leads to an even greater increment of the surface potential (difference between the black and red lines). The reason is that the saturation layer is mostly made of Na^+ ions close to the plane and Ca^{++} ions further away rather than just Ca^{++} ions when only steric interactions are taken into account. This reduces the saturation layer charge density so that it needs to be thicker in order to neutralize the surface charge.

4. Conclusion

We present a detailed account of the equilibrium diffuse double layer properties for a charged plane immersed in an aqueous electrolyte solution. We use an extension of the modified PB equation that takes into account the finite ion size by modeling the aqueous electrolyte solution as a suspension of polarizable insulating spheres in water, which leads to the following consequences [11]:

(1) The excluded volume occupied by the ions modifies the local value of the electrolyte solution permittivity.
(2) The resulting permittivity gradients lead to the appearance of a Born force that tends to move ions towards regions of higher permittivity.
(3) Ions get polarized by the local electric field and are acted upon by a dielectrophoretic force that is proportional to the field gradient.

We apply this formalism to a general electrolyte solution composed of two or more counterion species with different valences, sizes, and effective permittivity values. We show that the interplay of the electric, thermal, steric, Born and dielectrophoretic forces leads to rather unexpected effects in the three considered situations:

Case 1. Two univalent counterion types and equal bulk concentrations: 5 mM LiCl and 5 mM CsCl mixture. Instead of a saturation layer close to the plane evenly populated by Li^+ and Cs^+ ions a thicker layer made mostly of the smaller Cs^+ ions is predicted. This is mostly due to the dielectrophoretic force that repels counterions away from the charged plane and is proportional to the ion volume that is larger for the Li^+ ion.
Case 2. Two univalent counterion types and different bulk concentrations: 5 mM NaCl solution at pH = 4. Instead of a saturation layer close to the plane made almost exclusively of Na^+ ions, a broader layer with a high H^+ and a lowered Na^+ composition in the plane proximity is predicted. While this layer is

saturated, the total counterion concentration is no longer uniform increasing close to the interface because H^+ ions can be more densely packed than Na^+ ions. It should be noted that this behavior, mostly due to the dielectrophoretic force and its dependence on the ion size, is achieved despite the use of a steric interaction equation that does not favor the increase of the smallest ion concentration near the charged plane.

Case 3. One univalent and one divalent counterion type and equal bulk concentrations: 5 mM NaCl and 5 mM $CaCl_2$ mixture. Instead of a saturation layer close to plane made almost exclusively of Ca^{++} ions, a broader layer with a higher Na^+ than Ca^{++} concentration in the immediate proximity of the plane followed by a region where the Ca^{++} concentration amply surpasses that of Na^+, is predicted. Contrary to the two preceding cases, this behavior is mainly due to the dependence of the dielectrophoretic force on the effective ion permittivity (much smaller for divalent than univalent ions) rather than the ion size.

Besides these detailed changes in the double layer composition, there is a global change that is common to all the considered cases: the surface potential value strongly increases as compared to the modified PB theory that includes steric interactions among ions. This effect is particularly important in the case of mixtures of univalent and divalent counterions, being significant even for relatively low surface charge values.

Earlier works [7] have shown that when different size counterions are present in the system, the composition of the diffuse double layer can strongly differ from the classical prediction: smaller ions tend to come closer to the charged plane than larger ones and this effect can even overcome a difference in ion valences. However, this behavior was deduced using an expression for the activity coefficients that depends on the sizes of the different ion types [21] rather than the total volume excluded by all the ion types [5,20]. In this work we show that a similar behavior also occurs due to a totally different phenomenon: just the dependence of the Born and the dielectrophoretic forces on the ion sizes and effective permittivities. This suggests that the ion size effects reported to date, both in and out of equilibrium, are still strongly underestimated. A full theory incorporating activity coefficients that depend on the sizes of the different ion types together with all the forces related to the representation of the ions as dielectric spheres and considering, furthermore, that the minimum approach distances of ions to the interface must depend on the ion size, is required. This is a work in course that will be presented in the near future.

Acknowledgments

The authors wish to acknowledge financial support for this work provided by Ministerio de Economía y Competitividad (MICINN: Project FIS2010-19493) of Spain, co-financed with FEDER funds by EU, and by CIUNT (Project 26/E419) of Argentina.

References

[1] D. Andelman, Electrostatic properties of membranes: the Poisson-Boltzmann theory, in: R. Lipowsky, E. Sackmann (Eds.), Handbook of Biological Physics, vol. 1, Elsevier Science, Amsterdam, 1995 (Chapter 12).
[2] D.F. Evans, H. Wennerström, The Colloidal Domain, VCH Publishers, New-York, 1994.
[3] R.J. Hunter, Zeta Potential in Colloid Science. Principles and Applications, Academic Press, London, 1981.
[4] J. Lyklema, Fundamentals of Colloid and Interface Science, Solid/Liquid Interfaces, vol. II, Academic Press, London, 1995 (Chapter 3).
[5] J.J. Bikerman, Philos. Mag. 33 (1942) 384.
[6] M.Z. Bazant, M.S. Kilic, B.D. Storey, A. Ajdari, Adv. Colloid Interface Sci. 152 (2009) 48.
[7] P.M. Biesheuvel, M. van Soestbergen, J. Colloid Interface Sci. 316 (2007) 490.
[8] I. Borukhov, D. Andelman, H. Orland, Phys. Rev. Lett. 79 (1997) 435.
[9] K. Bohinc, V. Kralj-Iglic, A. Iglic, Electrochim. Acta 46 (2001) 3033.
[10] J.J. López-García, M.J. Aranda-Rascón, J. Horno, J. Colloid Interface Sci. 316 (2007) 196.
[11] J.J. López-García, C. Grosse, J. Horno, Langmuir 27 (2011) 13970.
[12] J.J. López-García, J. Horno, C. Grosse, J. Colloid Interface Sci. 380 (2012) 213.
[13] J.C. Maxwell, A Treatise on Electricity and Magnetism, vol. 1, Clarendon, Oxford, 1892.
[14] D. Ben-Yaakov, D. Andelman, R. Podgornik, J. Chem. Phys. 134 (2011) 074705.
[15] M.M. Hatlo, R. van Roij, L. Lue, Eur. Phys. Lett. 97 (2012) 28010.
[16] M. Born, Z. Phys. 1 (1920) 45.
[17] H.A. Pohl, J. Appl. Phys. 29 (1958) 1182.
[18] E.R. Nightingale, J. Phys. Chem. 63 (1959) 1381.
[19] S. Gavryushov, J. Phys. Chem. B 112 (2008) 8955.
[20] N.F. Carnahan, K.E. Starling, J. Chem. Phys. 51 (1969) 635.
[21] T. Boublík, J. Chem. Phys. 53 (1970) 471.
[22] G.A. Mansoori, N.F. Carnahan, K.E. Starling, T.W. Leland, J. Chem. Phys. 54 (1971) 1523.